Comparison between GMAT and ASW Special Perturbations Propagators

Trent Seelig, Daniel Topa

April 17, 2025

Abstract

The current operational standard for predicting orbits, within the United States Space Force, is the Astrodynamic Support Workstation Special Perturbations (ASW SP) propagator. One alternative to the ASW SP propagator that is open source and offers users more control is the General Mission Analysis Tool (GMAT). We perform a qualitative comparison of each of the GMAT propagators with the ASW SP propagator, comparing algorithmic speed and relative positional predictions. Additionally, we examine how these propagators compare with Global Navigational Satellite System (GNSS) operational data.

1 Introduction

The Astrodynamic Support Workstation (ASW) was developed by Omitron and introduced into operations with the United States Air Force in the late 90s, deployed on the Command, Analysis, Verification, and Ephemeris Network (CAVENet). A key element of ASW is the Special Perturbations (SP) algorithm, a highly accurate numerical orbital propagator. Today, ASW continues to be an important operational element and its SP algorithm has been held up as a standard through the Standardized Astrodynamic Algorithm Library (SAAL). For those that wish to use the ASW SP algorithm, access is controlled as it is proprietary and subject to government restrictions, which makes it difficult to work with.

Whereas ASW is proprietary and access to it is restricted, the General Mission Analysis Tool (GMAT) is open source and contributed to by a community of users. Initially developed in the early 2000s, it has since seen strong use within NASA and other academic and commercial groups. Additionally, GMAT has been used to support operations as well as design flight trajectories for several high profile NASA flight projects. This lends credence to GMAT that it may be capable of higher fidelity orbital propagation.

For users interested in a comparable alternative to ASW, GMAT may provide that option. Therefore, we seek to quantitatively evaluate the ASW SP propagator and each of the numerical propagators within GMAT, examining their speed and comparing their predicted orbits. Additionally, we also compare them with ephemeris from the Global Navigation Satellite System.

In the first section of this paper we perform a qualitative comparison of GMAT propagators with the ASW SP propagator. In the second section we perform a comparison of each propagators predictions when using operational GNSS data. For each test, we discuss the force models used as well as the particular sample of satellite(s).

2 GMAT vs ASW

2.1 Satellite Sample

For our comparison of GMAT and ASW propagators, we selected several satellites for their orbital parameters, with each selected to test a different orbital regime.

For orientation we summarize each satellite. Satellite 5567, Starlink 5708, is a commercial communications satellite; Satellite 41328, Navstar 76, is a GPS satellite in the GPS constellation; Satellite 42818, Intelsat 35e, is a high throughput communications satellite; Satellite 26936, Raduga 1, was a Russian military communication satellite moved into a graveyard orbit in 2015; Satellite 43013, JPSS-1, also known as NOAA-20, is a weather observation satellite; Satellite 9880, Molniya1-36, is a Russian communication satellite placed in a Molniya orbit.

In Table 1 we list each satellites, their NORAD ID, orbital type, and an estimation of their mass.

Table 1: Satellite Sample

LEO	MEO	GEO	HEO	POLAR	HighlyElliptical
Starlink 5708	NAVSTAR76 (GPS IIF-12)	Intelsat 35e	Raduga 1	JPSS-1 (NOAA-20)	Molniya 1-36
satNo 55470	satNo 41328	satNo 42818	satNo 2693	satNo 43013	SatNo 9880
306 Kg	1630 Kg	6761 Kg	2320 Kg	578 Kg	1600 Kg

2.2 Initial State Vectors and Epochs

Initial state vectors and their corresponding epoch are listed in Table 2. Each initial state vector was obtained from GNSS data and converted from the IGb14 coordinate system, which is similar to the ITRF coordinate system, to the geocentric celestial reference system (GCRS) using the Python package, *Astropy* (CITE IGb14 to ITRF and ASTROPY). Throughout our tests, we use *Astropy* to handle coordinate conversions and other operations necessary for our analysis.

Table 2: Initial State Vectors

satNo	55470	41328	42818
Epoch	9 May 2023 07:11:29.646	11 Mar 2024 22:00:00.000	09 May 2023 05:13:42.664
x km	4384.7929	-16917.5539	492.5447
y km	-3525.3536	15354.4382	-42168.3178
z km	4050.2238	13575.3476	-3.7369
$\dot{x}$ km/s	5.7822	-1.6866	3.0740
$\dot{y}$ km/s	4.1233	0.2997	0.0363
$\dot{z}$ km/s	-2.6647	-2.4985	0.0015

Initial State Vectors cont.

satNo	26936	43013	9880
Epoch	7 Mar 2023 20:19:42.498	9 May 2023 13:51:44.444	7 May 2023 07:09:07.155
x km	-38384.5788	2424.6988	-7396.3727
y km	-18976.2335	3813.0240	-9161.1557
z km	-678.4189	5605.3090	1324.0092
$\dot{x}$ km/s	1.3244	-1.4959	0.2533
$\dot{y}$ km/s	-2.6565	-5.7149	-4.1313
$\dot{z}$ km/s	-0.7143	4.5238	5.9299

2.3 Force Modelling

Our force models used in the comparison propagations between the GMAT propagators and ASW propagator only include gravitational models. For both propagators, we use the EGM96 spherical

harmonic geopotential model and include modelling for Earth, the Sun, and the Moon. GMAT treats the Sun and the Moon as point sources. For both GMAT and ASW, we truncate the order of the model to order 70 and in GMAT we specifically include relativistic corrections, assuming that ASW includes them as well. For both models we do not include tidal models.

2.4 Propagators

Unfortunately, due to its controlled nature, we know little about the ASW SP propagator beyond that it is a numerical propagator. Alternatively, we have a better understanding of the characteristics of the GMAT propagators. A survey of these characteristics is outlined in the GMAT documentation, which we summarize in Table 3.

Propagator	Integrator Name	Order	Error Control	Adaptive Step
ASW SP	Special Perturbations	-	-	-
GMAT PD45	Prince Dormand	Fifth	Fourth	Yes
GMAT PD78	Prince Dormand	Eighth	Seventh	Yes
GMAT PD853	Prince Dormand	Eighth	Fifth	Yes
GMAT RK56	Runge Kutta	Sixth	Fifth	Yes
GMAT RK68	Runge-Kutta-Nystrom	Eighth	Sixth	No
GMAT RK 89	Runge Kutta	Ninth	Eighth	Yes

Table 3: Propagators, For more details, users may refer to the GMAT Operators Manual(CREDIT GMAT MANUAL)

We propagate each state vector for 5 days from the epoch indicated and output the orbital prediction at a time resolution of 3 seconds. Each propagator is allowed to adaptively select the step size.

State vectors are propagated in a similar coordinate system for both GMAT and ASW. For both, we select a mean equatorial system mean epoch system referenced to the J2000 epoch. For GMAT, this is their MJ2000eq system and for ASW it is their MEME J2000 system. This coordinate system is

2.5 Performance Comparison

We compare the performance of each propagator with one another, examining how long each propagation took as well as the offset from each orbital prediction form GMAT with the complimentary ASW orbital prediction. It is important to note that any offset of one algorithm from the another doesn't indicate superior performance of one propagator versus the other. It is instead an indicator of the similarity of each algorithms predictions.

Propagator	LEO	MEO	GEO	HEO	POLAR	HighlyElliptical
ASW SP	5.262s	5.224s	5.165s	5.189s	5.214s	5.202s
GMAT PD45	15.201s	15.554s	15.374s	15.544s	15.783s	15.538s
GMAT PD78	23.509s	23.451s	23.463s	23.790s	23.791s	23.678s
GMAT PD853	22.214s	22.524s	22.335s	22.630s	22.673s	22.644s
GMAT RK56	16.772s	16.959s	17.005s	17.705s	17.039s	17.026s
GMAT RK68	17.898s	18.048s	18.179s	18.205s	18.079s	18.200s
GMAT RK89	27.585s	27.793s	27.879s	28.050s	27.731s	27.812s

Table 4: The total run time is measured as the wall clock time.

Our results in Tables 4 and 5 show that for each test each of the GMAT propagators were all within 10m of one another. The largest difference is attributabkle to predictions from the Runge-Kutta 68 propagator. For each orbital regime, offsets from each prediction with the ASW SP predictions were, mostly, no greater than 30m, with the single outlier again attributed to the Runge-Kutta 68 algorithm.

The run times for each test were also similar for each of the GMAT propagators. The longest run times were for the highest order integrators, PD78, PD853, and RK89 and the run times scaled with the order of the integrator. Variance for each propagator between orbital regimes was less than a

Propagator	LEO	MEO	GEO	HEO	POLAR	HighlyElliptical
ASW SP	-	-	-	-	-	-
GMAT PD45	23.7729m	8.0670m	8.1517m	21.7622m	2.6753m	20.8535m
GMAT PD78	23.7725m	8.0666m	8.1515m	21.7625m	2.6748m	20.8531m
GMAT PD853	23.7725m	8.0671m	8.1515m	21.7624m	2.6756m	20.8530m
GMAT RK56	23.7722m	8.0671m	8.1514m	21.7624m	2.6748m	20.8534m
GMAT RK68	33.4211m	8.3954m	8.1540m	21.7655m	5.5262m	21.8306m
GMAT RK89	23.7727m	8.0671m	8.1515m	21.7622m	2.6748m	20.8532m

Table 5: The offset in final position between each GMAT propagator and the ASW SP propagator is an indicator of how closely their relative predictions compare.

second. Comparitively, each run time for GMAT was an order of magnitude larger than the run times for the corresponding ASW predictions.

It should be noted that the *GMAT Reference Guide* also utilized performance tests for their algorithms. These tests varied in flight regime as well as propagation length and force models. These tests indicate positional agreeance between propagators similar to what we had found. However, when comparing their run times, they find the Prince Dormand 78 propagator to be the fastest algorithm in four of their six tests. This lack of agreeance between our test and theres is unclear but may be due to the different parameters spaces chosen.

3 Comparing ASW and GMAT Performance with GNSS Ephemeris

In addition to quantitatively comparing the set of GMAT and ASW propagators with one another, we have used each propagator to predict the orbit of a satellite in Medium Earth Orbit (MEO) using an initial state vector obtained from the GNSS. We are then able to compare the predicted orbital trajectory with orbital trajectories generated with GNSS ephemeris. This allows us to study how these propagators behave compared to operational data.

3.1 GNSS Ephemeris

We use an initial state vector for NAVSTAR 76, the MEO satellite, described in the previous section. Data for this object, obtained data from the Unified Data Library (UDL) (CITE UDL), has been produced by the MITRE Corporation from available GNSS broadcasts. We select ephemeris using an arbitrarily chosen epoch starting epoch for a period of 5 days. GNSS ephemeris contains positional data at a time resolution of 5 minutes. This data is expected to be of relatively exceptional accuracy with positional errors of the order of centimeters (cite IGS website).

	GNSS Initial SV	ASW Final SV	GMAT-PD78 Final SV
Epoch	1 Apr 2024 11:45:00.000	-	-
x km	5486.78160207	1248.15259203	1247.945377
y km	18258.08044214	17114.80877083	17114.946039
z km	-18196.93724089	-20007.03172096	-20007.345388
$\dot{x}$ km/s	-3.43654712	-3.53023839	-3.53019805
$\dot{y}$ km/s	-0.68298784	-1.14640996	-1.14641507
$\dot{z}$ km/s	-1.72171045	-1.20822327	-1.20818537

Table 6: We use an initial state vector for the NAVSTAR 76 satellite obtained from GNSS data. We list below the initial state vector and the final state vectors of predicted trajectories

3.2 Force Modelling and propagation

To understand how well GMAT and ASW propagators orbital predictions compare with real data we include force models from massive bodies, atmospheric drag, as well as Solar Radiation Pressure (SRP). For consistency, we utilize the same gravitational model as we previously described in our quantitative

comparison of GMAT and ASW. We also use SRP models and atmospheric pressure models that are common to both GMAT and ASW and attempt to specify common physical parameters to describe the satellite. We use the mass for NAVSTAR 76 that we have listed in Table 1.

GMAT allows users to set the dimensionless coefficients of drag (C_d) and reflectivity (C_r), which we set to be 2.2 and 1.8, respectively. It also allows users to set the effective drag area and the SRP area, which we set both be 15 m^2.

ASW allows for less freedom to specify parameters, and instead only allows users to specify the ballistic coefficient and radiation pressure coefficient. We calculate the ballistic coefficient using equation 1 and our assumed constants.

$$C_{bal} = \frac{m}{C_d A} \tag{1}$$

Without a clear understanding how ASW has defined their radiation pressure coefficient, we set it equal to the coefficient of reflectivity we used for GMAT.

For both GMAT and ASW propagations add to the force model a drag component based on the Jacchia-Roberts atmospheric drag model. This model defines a density and temperature model that is considered valid above 90 km (CITE JR PAPER). For both GMAT and ASW, we set the value for the solar radio flux at 10.7 cm and the average value at 10.7 cm (F107 and F107A respectively) to be 150 and the magnetic index to be 3. Finally, we also add to the force model an SRP component. We hold the flux values to be constant and for GMAT we specify a flux value of 1367 $\frac{W}{m^2}$ at a specified distance to the sun of $1.49597870691 \times 10^8$ km. In ASW we set the flux level to be "constant", but it is not immediately clear what this constant value is.

We use a similar set of propagators as we had previously used but unlike our previous test we propagate our state vectors and record output at a time resolution that equivalent to the GNSS dataset, at 5 minute intervals.

3.3 Results

We have compared each of the GMAT and ASW propagators to operational data. We show a comparison of performance in 1. Between GMAT and ASW, their relative positional offset grows with time. It is likely that this offset can be attributed to the assumptions we needed to make regarding the ASW force model. Improperly implementing the force model could lead to a growth in offset similar to what we see in Figure 1a.

Their RMSE, compared with the GNSS data set, also grows at a similar rate until it begins to diverge at about 3.7^9 sec. In 2, the relative growth of the RMSE of the GMAT PD-78 propagator with each of the other GMAT propagators shows they behave similarly until about 3.7^9 sec but overall they differ by less than a meter. For all propagators, over the five day propagation period, we find their RMSE growth to be within 5 km.

4 Conclusion

The relative performance of each of the GMAT and ASW propagators suggests their predictions are in agreeance within 1 meter. Differences between GMAT and ASW orbital predictions, when seeded with state vectors from GNSS data, are also within a kilometer of one another. Assuming the force model was incorrectly implemented for ASW, this difference would decrease and the predictions would be within 25 meters of one another.

It is important to note that the comparison of GMAT and ASW predictions with GNSS operational data sampled only a single orbital regime and only one state vector. It is possible that ASW or GMAT may offer superior or inferior force modelling, which may become increasingly obvious at lower altitudes we did not test. It is also possible that their longer term predictions may be more or less accurate than one another.

Indeed the largest difference between GMAT and ASW propagators appears to be their run times, with GMAT propagations taking 10-20 seconds longer than the ASW propagations. Therefore, the algorithmic speed may be the most important difference. Overall these tests suggest similar performance between ASW and GMAT in terms of positional predictions and the only clear advantage of ASW is a faster algorithm. However, it is very possible that with further insight into the GMAT propagation algorithms, their speed may be increased.

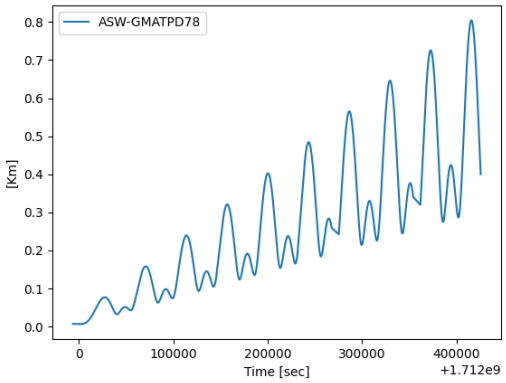

(a) Difference in magnitude of position between ASW and GMAT-PD78.

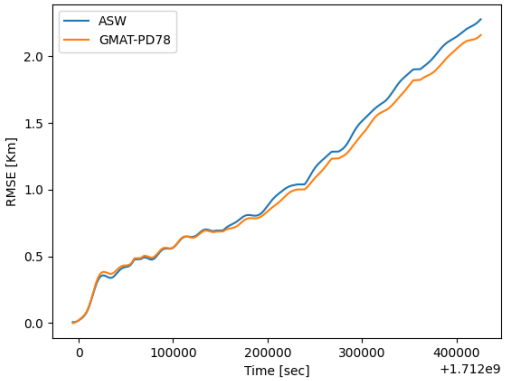

(b) Growth of RMSE for ASW and GMAT-PD78.

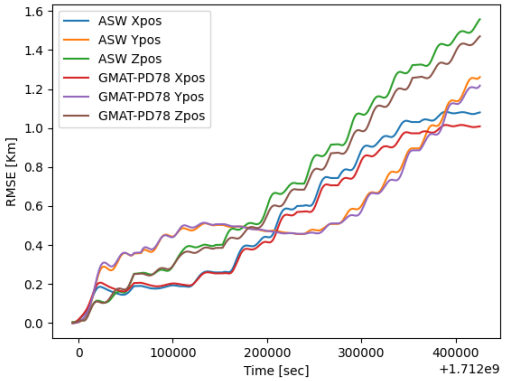

(c) Axis dependent growth of RMSE for ASW and GMAT-PD78.

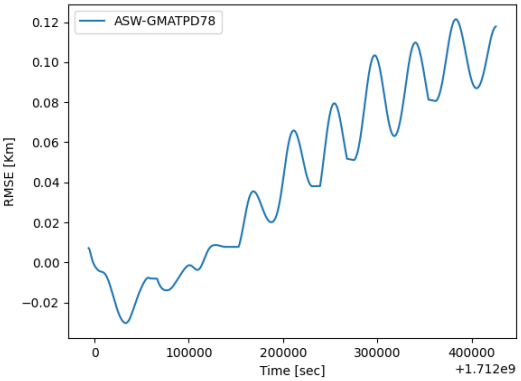

(d) Difference between ASW RMSE growth and GMAT-PD78 RMSE growth.

Figure 1: Positional offset between the ASW SP predictions and the GMAT-PD78 predictions grow with time. Additionally, the RMSE between ASW and GNSS as well as GMAT and GNSS data grows with time. Notably, the rate of growth changes for both predictors at about 3.7×10^9 sec. While one data point is not necessarily an indicator of accuracy, the trend of similar behavior between both predictors suggests similar performance for Medium Earth Orbit predictions.

References

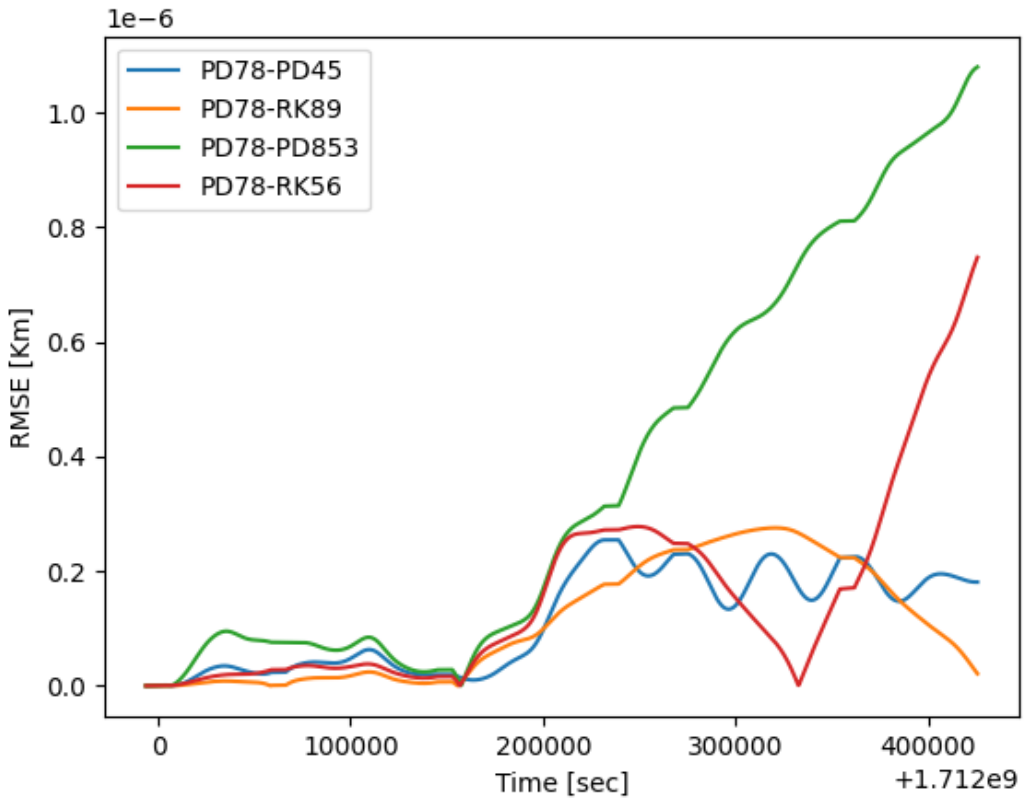

Figure 2: The difference of RMSE growth between orbits predicted with the GMAT PD78 propagator compared with each of the other GMAT propagators shows a similar point of divergence to what we had seen when we compared the GMAT PD78 propagator with the ASW SP propagator. Each of the GMAT propagators differ by less than a meter relative to one another, which is in agreeance with what we had seen when qualitatively comparing their performance.